



UDC 621.398

Cascade frequency converters control features

Aleksei G. VORONTSOV¹, Vasilii V. GLUSHAKOV², Mikhail V. PRONIN¹, Yuriy A. SYCHEV³✉

¹ Saint Petersburg Electrotechnical University, Saint Petersburg, Russia

² PJSC “Power mashines”, Saint Petersburg, Russia

³ Saint Petersburg Mining University, Saint Petersburg, Russia

The structures of systems with high-voltage cascade frequency converters containing multi-winding transformers and low-voltage low-power converters connected in series at each output phase of the load are considered. Low-voltage blocks contain three-phase diode or active rectifiers, DC capacitor filters, single-phase stand-alone voltage inverters and block disconnecting devices in partial modes (in case of failure when part of the blocks are disconnected). The possibilities of operation of cascade converters are determined, equations for correcting tasks to units in partial modes are given, tables of correction of tasks with estimates of achievable load characteristics are proposed. The results of experiments on the model of a powerful installation with a cascade frequency converter are presented, confirming the possibility of ensuring the symmetry of the load currents when disconnecting part of the blocks and the asymmetry of the circuit.

Key words: cascade frequency converter; diode rectifier; active rectifier; single-phase inverter; symmetry of the currents; control algorithm; experiment

How to cite this article: Vorontsov A.G., Glushakov V.V., Pronin M.V., Sychev Yu.A. Cascade frequency converters control features. Journal of Mining Institute. 2020. Vol. 241, p. 37-45. DOI: 10.31897/PMI.2020.1.37

Introduction. Powerful semiconductor frequency converters (FC) are widely used in enterprises of the mineral raw materials complex [1, 3-5, 7, 8]. They are used in electric drives of mills, fan drives for main ventilation of mines [8], excavators, heavy-duty dump trucks [7], mine hoists, pump drives, drilling rigs, etc. As an example, it can be noted that more than 700 frequency-controlled electric drives with high-voltage drives with a capacity of 4 to 12.5 MW are used on Russian gas pipelines [5]. Of the many types of inverters, cascade frequency converters (CFC) are most in demand. CFC are supplied by many well-known companies – Siemens AG (Sinamics perfect harmony GH180 converters), Toshiba Mitsubishi-Electric (TMdrive-MVe2 converters), Hyundai (N5000 converters), etc.

Cascading frequency converters are built using low-voltage transistor-based converters (TBC) with a single-phase output. The CFC usually includes a transformer (Tr), which has a three-phase primary winding and several secondary windings. Each TBC receives power from an individual secondary winding Tr. In each phase of the CFC load, low-voltage TBCs are connected in series and form a high-voltage three-phase power supply with adjustable voltage and frequency. The load of the inverter can be synchronous or asynchronous machines or other devices. CFC is usually performed at voltages of 3, 6, 10 kV, etc.

The widespread use of the CFC is due to the following advantages:

- slight distortion of voltages and currents at the input and output of the CPC, which allows to apply them without additional filters;
- the ability to build high-voltage installations on low-voltage elements;
- ample opportunities to reserve semiconductor elements and ensure the operability of systems in case of failure of some elements [8, 15].

The article discusses the structure of the CFC and their capabilities to ensure the specified modes of operation in case of failure of part of the semiconductor elements.

The structures of electric drives with a CFC are determined by a given power, input and output voltages, energy recovery requirements, the nature of the load (fan drive, propeller, rolling mill, hoist), other requirements (efficiency, reliability, survivability, cyclic stability of IGBT-modules), element base (voltage and current of IGBT-modules, diodes, capacitors, etc.).

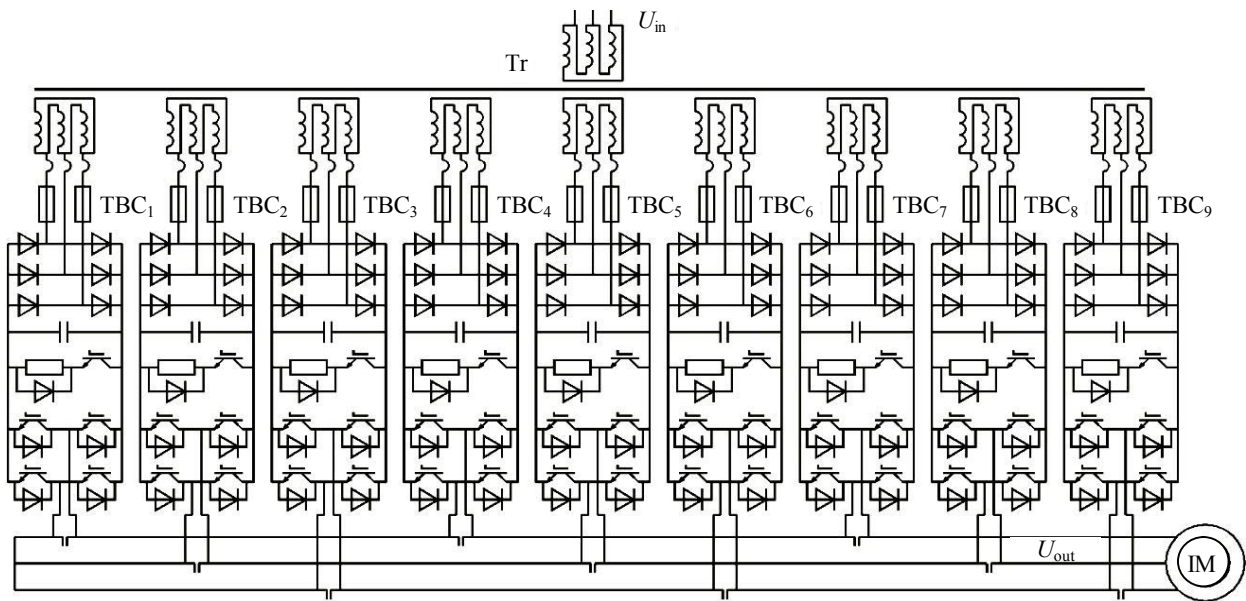


Fig.1. The installation scheme of the CFC and TBC with diode rectifiers

If energy recovery of the motors through the CFC is not required to the supply network, then diode rectifiers are used in low-voltage TBC. To reduce distortion of currents and network voltages, a multi-winding transformer is used, in which the secondary windings are mutually shifted in phase. The drive circuit with a 10-winding transformer and a converter with nine low-voltage TBCs with diode rectifiers is shown in Fig.1.

In the circuit (Fig.1) in the phases of the power supply circuit of an induction motor (IM) three TBCs are connected in series. The mutual phase shift of the triples of the transformer secondary windings is performed at angles that are multiples of π/N , where N is the number of TBC in the CFC. In the circuit, every three secondary windings of the transformer coincide in phase, and these three windings are made with phase shifts relative to the network voltage by angles of $-20, 0, +20$ degrees, which corresponds to an 18-pulse rectification circuit. Each TBC contains a three-phase diode rectifier, a DC capacitor filter, a protection circuit against an increase in the rectified voltage with a chopper and a resistor, as well as a single-phase autonomous voltage inverter (AVI). As part of the TBC, fuses in the rectifier phases and a switching device at the output of the AVI can be used. With these elements, the unit is excluded from operation when it malfunctions. The remaining operating TBC provide the specified mode of operation of the CBC.

Recovery of IM energy into the supply network is not possible, since diode rectifiers are used in the CFC. However, part of the energy of IM can be returned through the AVI in the circuit of the rectified current and spent in the resistors of the protective circuits. If the drive requires recovery of significant energy (mine hoists, etc.), then in the TBC rectifiers are active, for example, on IGBT modules [2, 6-10].

CFC control algorithms in normal operation. Algorithms for controlling multilevel frequency converters are considered in many publications [8, 13, 14]. In the considered CFC control systems (CS) of automatic circuit breaker (ACB) and AVI can be performed with independent control from each other [2, 7]. In the control system of single-phase AVIs, transistor control pulses are generated as a result of comparing the control voltage u_y with the reference voltages u_{om} (m is the number of BPC in the phase). If several TBCs are used in the load phase (for example, 2, 3, 4 or 5), then there are several reference voltages, as shown in Fig.2.

In the normal mode of operation of the CFC, all sawtooth voltages have the same amplitude of ripple. Moreover, they are offset in level relative to each other so that the minima of some of the saws correspond to the maxima of the other saws. The instantaneous values of all saws are within ± 1 p.u. A single saw-tooth pulses family is used to control all TBCs. In each phase of the load, the control pulses of each AVI are assigned to a specific saw. The formation of transistor control pulses

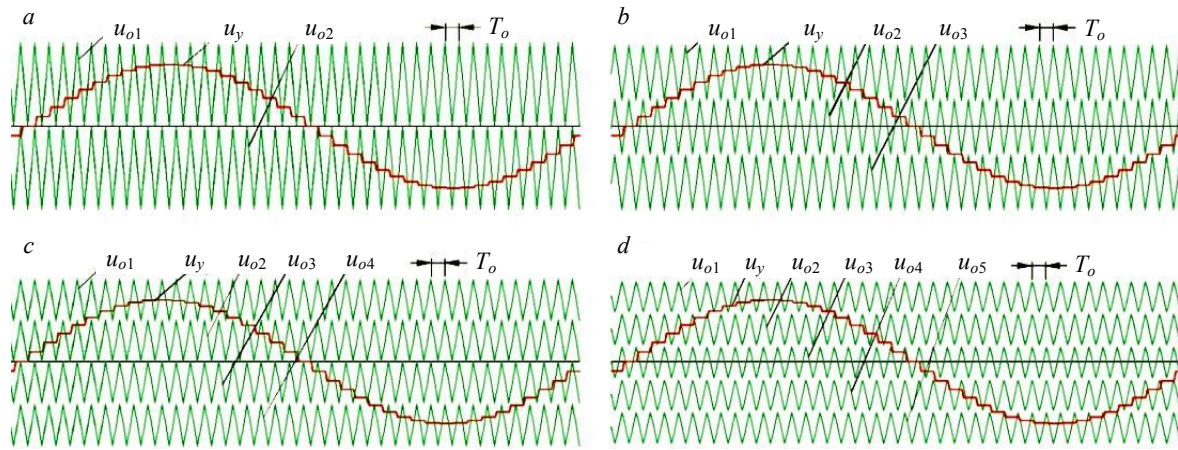


Fig.2. Support and control voltages of the CFC with two TBCs (a), three (b), four (c), five (d)

of any AVI is carried out as a result of comparing the phase control voltage with the reference voltage system of this AVI. At each moment of time in the PWM mode, only one AVI operates in each phase of the load, other AVIs of this phase are in overmodulation mode. It is also possible that all AVIs of this phase are in overmodulation mode.

Features of the operation of the CFC when disconnecting part of the TBS. In the event of a failure of the part of the TBC, the remaining blocks in the work create a symmetrical three-phase system of load voltages. If the voltage or current reserves are not provided for in the CFC, then the voltage and load power are reduced.

If in each phase of a three-phase load the number of TBCs is equal to m , then the total number of states of the CFC during operation of all TBCs or their parts is determined by

$$M = (m + 1)^3. \quad (1)$$

For a CFC with three TBCs in each phase of the load, the total number of CFC states is $M = 64$. Data on the CFC states, depending on the number of operational TBCs, are shown in Table 1.

Table 1

Mutual phase shifts and CFC load voltage with nine TBCs depending on the number of serviceable units

N	1	2	3	N	1	2	3	N	1	2	3	N	1	2	3	N	1	2	3	N	1	2	3	N	1	2	3	N	1	2	3	N	1	2	3				
		α_{12}	α_{13}			α_{12}	α_{13}			α_{12}	α_{13}			α_{12}	α_{13}			α_{12}	α_{13}			α_{12}	α_{13}			α_{12}	α_{13}			α_{12}	α_{13}			α_{12}	α_{13}				
1	3	3	3	9	3	1	3	17	2	3	3	25	2	1	3	33	1	3	3	41	Shift to	49	60	120	57	Shift to	59	0	1	3									
		120	240			140	281			131	229			238	300			140	220			Shift to					Shift to												
		$U = 100\%$				$U = 73.6\%$				$U = 87.8\%$				$U = 51.3\%$				$U = 73.6\%$			N 42					N 59													
2	3	3	2	10	3	1	2	18	2	3	2	26	2	1	2	34	1	3	2	42	1	1	2	50	Shift to	58	0	1	2										
		99	229			62	299			101	203			136	271			61	121			120	60			Shift to	Shift to												
		$U = 87.8\%$				$U = 51.6\%$				$U = 75.5\%$				$U = 53.9\%$				$U = 51.2\%$			N 54					N 59													
3	3	3	1	11	3	1	1	19	2	3	1	27	2	1	1	35	1	3	1	43	1	1	1	51	Shift to	59	0	1	1										
		79	220			Shift to				60	120			62	298			Shift to				120	240			Shift to	Shift to												
		$U = 73.6\%$				N 27				$U = 50.9\%$				$U = 33.9\%$				N 39				$U = 57.7\%$			N 59														
4	3	3	0	12	3	1	0	20	2	3	0	28	2	1	0	36	1	3	0	44	1	1	0	52	Shift to	60	0	1	0										
		60				Shift to				Shift to				Shift to				Shift to				60				Shift to	Stop	Stop											
		$U = 57.7\%$				N 44				N 24				N 44				N 44				$U = 19.2\%$																	
5	3	2	3	13	3	0	3	21	2	2	3	29	2	0	3	37	1	2	3	45	1	0	3	53	Shift to	61	0	0	3										
		131	261			300				157	259			Shift to				121	61			Shift to				Shift to	Shift to												
		$U = 87.8\%$				$U = 57.7\%$				$U = 75.5\%$				N 30				$U = 51.2\%$				N 47				N 54													
6	3	2	2	14	3	0	2	22	2	2	2	30	2	0	2	38	1	2	2	46	1	0	2	54	Shift to	62	0	0	2										
		101	259			Shift to				120	240			300				136	225			Shift to				Shift to	Shift to												
		$U = 75.5\%$				N 30				$U = 66.7\%$				$U = 38.5\%$				$U = 53.8\%$				N 47				N 54													
7	3	2	1	15	3	0	1	23	2	2	1	31	2	0	1	39	1	2	1	47	1	0	1	55	Shift to	63	0	0	1										
		61	298			Shift to				89	224			Shift to				60	120			Shift to				Shift to	Shift to												
		$U = 51.6\%$				N 47				$U = 53.9\%$				N 47				$U = 33.3\%$				N 59				N 59													
8	3	2	0	16	3	0	0	24	2	2	0	32	2	0	0	40	1	2	0	48	1	0	0	56	Shift to	64	0	0	0										
		Shift to				Stop				60				Stop				Shift to				Stop				Stop	Stop	Stop											
		N 24								$U = 38.5\%$								N 44				Stop			Stop	Stop	Stop												

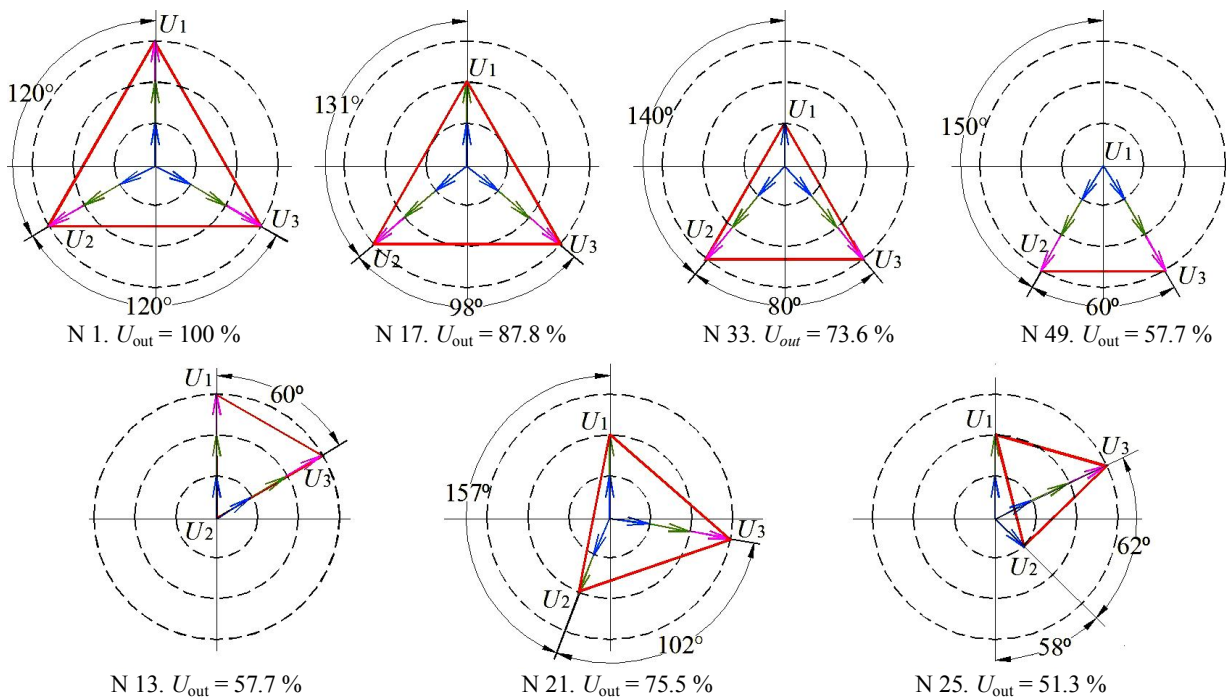


Fig.3. The formation of a three-phase symmetric voltage system at the output of the CFC with nine TBCs in case of failure of part of the TBC

The top row of the table shows the phase numbers. The second line at the top shows the designation of the angles of shift of the stress vectors of the 2nd and 3rd phases of the CFC relative to the 1st phase (α_{12} and α_{13}). Columns with the headings “N” indicate the status numbers of the CFC. In the other rows of Table 1, the number of operational BPFs in each load phase is indicated, as well as those phase shifts of the stress vectors (in degrees) relative to the 1st phase vector, at which the symmetry of the three-phase system of load voltages is ensured with the maximum use of operating TBC. The highest symmetrical load voltages, which are provided by serviceable TBCs, are also indicated. The operating states of the CFC are shown on a light background, the gray background shows the states from which it is necessary to switch to the operating states (for example, from state N 12 to state N 33), against a dark background – shutdown the unit (Stop).

For a CPC with nine TBCs, some states of the system are shown in Fig.3 in the form of phase voltage diagrams during the formation of a three-phase symmetric system of load voltages (depending on the number of operational BPCs).

If the CFC contains 15 TBCs (5 each in the load phases), then the state of the system, depending on the number of operational TBCs in phases, is presented in Table 2. The system states are numbered, the permissible ones for operation are indicated (on a light background).

Figure 4 under N 1 shows a vector diagram of the phase voltages during operation of all TBCs. Angles of mutual shift of vectors is 120 deg. The stress phase vector of the load is formed as the sum of the stress vectors of the operating AVI. The lines connecting the ends of the phase voltage vectors form a symmetrical three-phase system of load voltages (100 %).

Fig.4 under N 37 shows the voltage diagram when disconnecting one TBC in the 1st phase of the load. The creation of a symmetric system of linear load voltages is provided by changing the phases of the 2nd and 3rd stress vectors (the angle of mutual shift of the 2nd and 3rd vectors is shown in Fig.4 – 107 electric degrees). In this case, the effective value of the symmetric system of linear load stresses decreases to approximately 93 %.

When three TBCs in the 1st phase and two TBCs in the 2nd phase (N 121) are disconnected, the CFC can form a symmetrical system of load voltages with an effective value of up to 53.6 %.

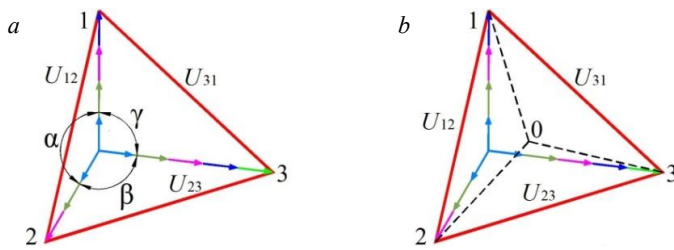


Fig.5. Phase and line voltage diagrams for the state of the TBC N 49

AVIs, as shown in Fig.2, c, in other phases; five reference voltages are used. If in the first phase of the load three TBCs remain in operation, then the number of reference voltages in the AVI of this phase decreases to three, as indicated in Fig.2, b.

With an unequal number of operating TBCs in phases, the angles change by which the phase voltage vectors are mutually shifted during the formation

of a symmetric system of linear voltages. These shear angles are determined using the diagram (Fig.5, a). In this case, the stresses of the phases of the load and the position of point 0 change (Fig.5, b).

Equations for a symmetric three-phase linear load voltage system:

$$|U_{12}| = |U_{23}|, \quad |U_{12}| = |U_{31}|, \quad (2)$$

where U_{12}, U_{23}, U_{31} – Line voltages RMS values.

Equations (2) can be written using phase voltages U_1, U_2, U_3 and the angles between them α, β, γ (phase voltages are proportional to the number of operating TBC):

$$\left. \begin{aligned} U_1^2 + U_2^2 - 2U_1U_2 \cos \alpha &= U_2^2 + U_3^2 - 2U_2U_3 \cos \beta; \\ U_1^2 + U_2^2 - 2U_1U_2 \cos \alpha &= U_3^2 + U_1^2 - 2U_3U_1 \cos \gamma; \\ \alpha + \beta + \gamma &= 2\pi. \end{aligned} \right\} \quad (3)$$

The system of equations (3) can be solved with respect to unknown angles α, β, γ by iterative methods, for example, in the next record of equations:

$$\left. \begin{aligned} \alpha_{n+1} &= (\alpha_n + Z\alpha_n + U_3^2 - 2U_2U_3 \cos \beta_n - U_1^2 + 2U_1U_2 \cos \alpha_n) / (1 + Z); \\ \beta_{n+1} &= (\beta_n + Z\beta_n + U_3^2 - 2U_3U_1 \cos \gamma_n - U_2^2 + 2U_1U_2 \cos \alpha_n) / (1 + Z); \\ \gamma_{n+1} &= 2\pi - \alpha_{n+1} - \beta_{n+1}, \end{aligned} \right\} \quad (4)$$

where n – iteration number; Z – parameter ensuring stability of the calculation process.

Not all CFC states can determine the angles $\alpha, \beta,$ and γ . For example, in case of a malfunction of all TBCs in two load phases in accordance with Table 1, system states N 16, 32, 48, 52, 56, 60, 61, 62, 63, 64 are impossible.

As a result of solving equations (4), using the known phases $\alpha, \beta,$ and γ and CFC voltages U_1 and U_2 , the highest load stresses with zero point 0 are determined (Fig.5, b):

$$U_1 = \sqrt{U_1^2 + U_2^2 - 2U_1U_2 \cos \alpha}; \quad U_r = U_1 / \sqrt{3}. \quad (5)$$

The voltages defined by expressions (5) should be considered as the voltage limitations at the output of the CFC that acts in the control system. Actual voltages may be less and are determined by the regulation system. The task of iterative calculation of phases and stresses by formulas (4) and (5) is solved in Excel.

Coordination of the characteristics of the CFC and the load in partial modes. If the load of the CFC is a synchronous motor, and the CFC does not provide a margin for output voltage, then when a part of the TBC is turned off, the motor voltage should be reduced, for example, by reducing the magnetic flux of the motor. While maintaining the load power, this leads to an increase in the currents at the output of the CFC, i.e. the equipment must have a current margin.

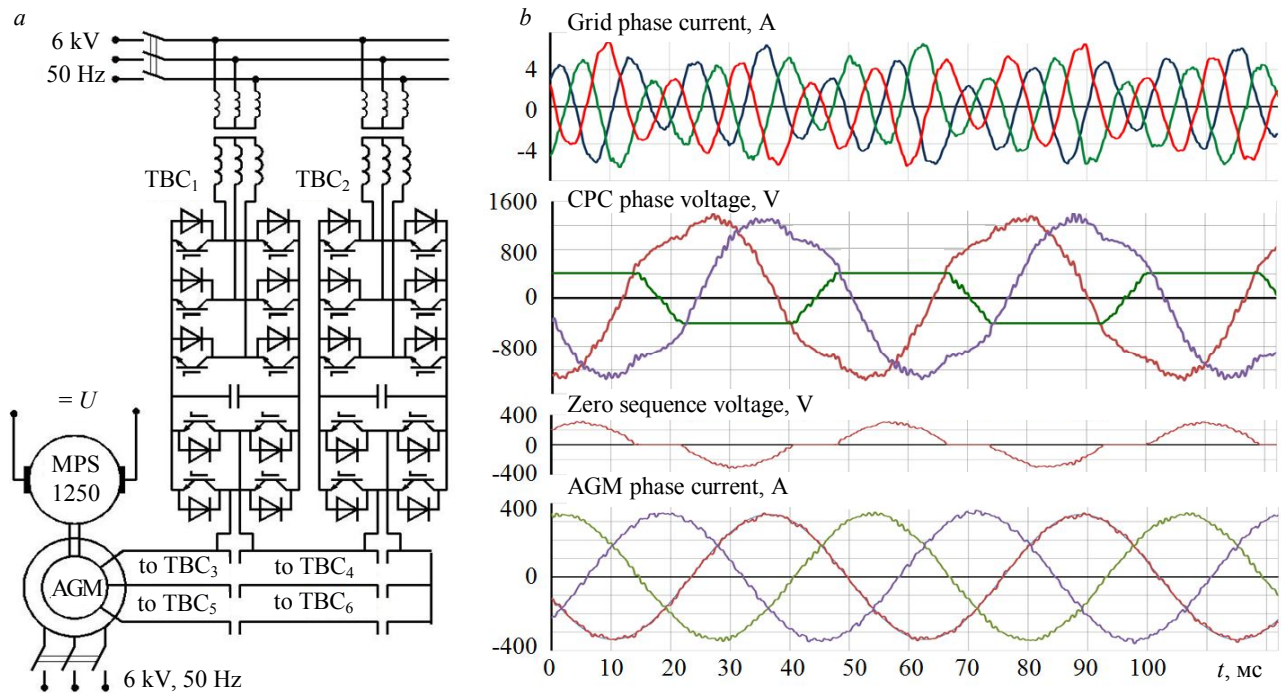


Fig.6. Layout diagram with a frequency converter, voltage and currents of a frequency converter when disconnecting one TBC₆

Another solution is that the voltage reserve is provided in the CFC. For example, in the CFC with active rectifiers, when the part of the TBC is turned off, the rectified voltages increase and due to this, the output voltages are supported.

Experimental research. An experimental verification of the considered technical solutions was carried out at PJSC “Power machines” on the layout of the installation containing an asynchronous generator-motor (AGM) with a three-phase rotor and an active CFC, which is connected to the rotor through slip rings. The stator of AGM is connected to the power supply network of 6 kV, 50 Hz. CFC inputs are connected to the same electric network through transformers. A simplified layout diagram is shown in Fig.6, *a*. AGM has a power of 2530 kVA. Sliding is adjustable within $\pm 40\%$. In the CFC in each phase of the load two TBCs are connected in series. PWM frequency of CFC is 4 kHz. The installation is equipped with a vector control system that supports a given operating mode of the installation, creating a three-phase symmetrical system of currents in the AGM rotor.

One of the research objectives is to evaluate the capabilities of the CFC and the control system for creating a symmetric system of currents in the AGM rotor in various modes when a part of the TBCs is turned off. Fig.6, *b* shows a diagram of the currents and voltages of the installation when the TBC₆ is turned off in the third phase. In this mode, the AGM slip is 40%. The instantaneous values of the variables are shown in Fig.6, *b*. In this case, the following control option is used. With an increase in the rotor voltage, TBC₅ cannot create the required phase voltage, since TBC₆ is turned off, and TBC₅ goes into overmodulation mode – its control voltage exceeds 1 p.u. In the control system, a portion of the control voltage of the TBC₅, exceeding 1 p.u., is remembered as a component of the zero sequence, which is subtracted from the control voltages of all phases. The resulting voltages are used as modified control voltages. Corresponding to the form of the modified voltages, the shape of the power phase voltages at the output of the CFC changes – the symmetry of the power stresses is lost, but the symmetry of the rotor currents is ensured, as can be seen from Fig.6, *b*).



In particular, the voltages of the 1st and 2nd phases are mutually shifted by less than 90 deg. (instead of 120 electric degrees in symmetrical modes).

It should be noted that in the asymmetric mode of operation of the CFC, the phase currents of the supply network are distorted. It should be expected that with a larger number of TBCs as part of the CFC, disconnection of one unit will lead to less distortion of the grid current.

Conclusions. Cascade frequency converters make it possible to create high-voltage systems using low-voltage power units. They have small distortions of currents and voltages at the input and output, provide galvanic isolation of power networks and loads, have high survivability, and allow adjusting the engine speed in the full range. Due to these advantages, cascade converters are widely used in the drives of gas line compressors, mine fans, pumps, in mine hoists, and in many other installations.

To implement effective control algorithms and increase the reliability and survivability of drives with cascade frequency converters, the analysis of the operating modes and characteristics of the converters in partial modes (in case of failure and disconnection of a different number of power units) is performed. It was revealed that for the formation of a symmetric system of load currents, it is necessary to correct tasks for the mutual shift of the phase voltage vectors depending on the number of working blocks. The state tables of converters are proposed, which determine the tasks by phase of the voltages, characterizing the possibilities of creating a symmetric three-phase system of load voltages in partial modes. The algorithm for calculating the settings for the phases of the voltage was mathematically determined.

On the breadboard installation with an asynchronized generator-motor with a power of 2530 kVA and an active cascade frequency converter of comparable power, experiments were performed confirming the effectiveness of the considered technical solutions. The converter control system uses a relatively simple algorithm for adjusting the phases of the output voltage in partial modes, based on the conversion of a part of the control voltage that goes beyond the reference voltage into a zero-sequence component and in the subtraction of this component from all phase control voltages. The implementation of this algorithm made it possible to ensure an almost sinusoidal shape of the phase currents at a PWM frequency of the converter 4000 Hz.

REFERENCES

1. Egorov A.N., Semenov A.S., Fedorov O.V. Practical experience with POWER FLEX 7000 frequency inverters in the mining industry. *Trudy NGTU im. R.E.Alekseeva*. 2017. N 4 (119), p. 86-93 (in Russian).
2. Efimov A.A. Active converters in variable AC drives. Novouralsk: Izd-vo NGTI, 2001, p. 250 (in Russian).
3. Kozyaruk A.E. Energy efficient electromechanical systems of mining and transport machines. *Zapiski Gornogo instituta*. 2016. Vol. 218, p. 261-269 (in Russian).
4. Kryukov O.V. Automated electric drive of turbochargers with high-voltage multilevel frequency converters. *Avtomatizatsiya i IT v energetike*. 2019. N 5 (118), p. 5-9 (in Russian).
5. Kryukov O.V. Analysis of structures of frequency converters for technologically connected electric drive gas pumping units. *Elektrotekhnicheskie sistemy i komplekсы*. 2015. N 2 (27), p. 11-14 (in Russian).
6. Pronin M.V., Vorontsov A.G. Power fully controlled semiconductor converters (modeling and calculation). St. Petersburg: Elektrosila, 2003, p. 172 (in Russian).
7. Pronin M.V., Vorontsov A.G., Tereshchenkov V.V. Control of multi-cycle active rectifier of excavator EKG-35K. *Gornoe oborudovanie i elektromekhanika*. 2009. N 10, p. 29-33 (in Russian).
8. Pronin M.V., Vorontsov A.G. Electromechatron complexes and their modeling according to interconnected subsystems. St. Petersburg: Ladoga, 2017, p. 220 (in Russian).
9. Shreiner R.T., Kalygin A.I., Krivovyaz V.K. Construction of high-voltage regenerative cascade direct frequency converters for electric drive. *Elektrotehnika*. 2012. N 9, p. 8-13 (in Russian).
10. Pronin M.V., Vorontsov A.G., Kalachikov P.N., Emelyanov A.P. Electric drives and systems with electric machines and semiconductor converters (modeling, calculation, application). St. Petersburg: Silovye mashiny. Elektrosila. 2004, p. 252 (in Russian).
11. Boonmee C., Kumsuwan Y. Control of single-phase cascaded H-bridge multilevel inverter with modified MPPT for grid-connected photovoltaic systems. IECON 2013. 39th Annual Conference of the IEEE Industrial Electronics Society. IEEE. Vienna. Austria. 2013. N 14016134.



12. Carnielutti F, Pinheiro H. New modulation strategy for asymmetrical cascaded multilevel converters under fault conditions. IECON 2013. 39th Annual Conference of the IEEE Industrial Electronics Society. IEEE. Vienna. Austria. 2013. N 14016058.
13. Ghoreishy H., Yazdian A.V. A new selective harmonic elimination pulse-width and amplitude modulation (SHE-PWAM) for drive applications. IECON 2013. 39th Annual Conference of the IEEE Industrial Electronics Society. IEEE. Vienna. Austria. 2013. N 14016018.
14. Rodríguez J, Lai J.-S., Peng F.Z. Multilevel inverters: a survey of topologies, controls, and applications. *IEEE Transactions on Industrial Electronics*. 2002. Vol. 49. Iss. 4, p. 724-738.
15. Rodríguez J., Pontt J., Musalem R., Hammond P. Operation of a medium-voltage drive under faulty conditions. *IEEE Transactions on Industrial Electronics*. 2005. Vol. 52. Iss. 4, p. 1080-1085.

Authors: **Aleksei G. Vorontsov**, Candidate of Engineering Sciences, Assistant Lecturer, ag.vorontsov@npcses.ru (Saint Petersburg Electrotechnical University, Saint Petersburg, Russia), **Vasili V. Glushakov**, Engineer, glushvas@yandex.ru (PJSC "Power mashines", Saint Petersburg, Russia), **Mikhail V. Pronin**, Doctor of Engineering Sciences, Professor, mpronin1@rambler.ru (Saint Petersburg Electrotechnical University, Saint Petersburg, Russia), **Yuriy A. Sychev**, Candidate of Engineering Sciences, Associate Professor, Sychev_YuA@pers.spmi.ru (Saint Petersburg Mining University, Saint Petersburg, Russia).

The paper was received on 31 March, 2019.

The paper was accepted for publication on 03 July, 2019.